SYNTHESES, SPECTROELECTROCHEMISTRY AND PHOTOINDUCED ELECTRON-TRANSFER PROCESSES OF NOVEL Ru AND Os DYAD AND TRIAD COMPLEXES WITH FUNCTIONALIZED DIIMIDE LIGANDS

M. Delower HOSSAIN[a], Masa-aki HAGA[a1,*], Bobak GHOLAMKHASS[b], Koichi NOZAKI[b1], Minoru TSUSHIMA[b], Noriaki IKEDA[b2] and Takeshi OHNO[b3]

[a] *Department of Applied Chemistry, Faculty of Science and Engineering, Chuo University, 1-13-27 Kasuga, Bunkyo-ku, Tokyo 112-8551, Japan; e-mail:* [1] *mhaga@apchem.chem.chuo-u.ac.jp*

[b] *Department of Chemistry, Faculty of Science, Osaka University, Machikaneyama, Toyonaka, Osaka 560, Japan; e-mail:* [1] *nozaki@ch.wani.osaka-u.ac.jp,* [2] *ikeda@ch.wani.osaka-u.ac.jp,* [3] *ohno@ch.wani.osaka-u.ac.jp*

Received November 8, 2000
Accepted January 20, 2001

This paper is dedicated to the memory of the late Professor Antonín A. Vlček. We will always remember his pioneering work, particularly in electrochemistry and spectroelectrochemistry of a wide range of transition metal complexes.

A series of mono- and dinuclear Ru complexes containing a bridging ligand, L-diimide-L (L = 2-(2-pyridyl)benzimidazole; diimide = benzene-1,2:4,5-bis(dicarboximide) (bdi; pyromellitimide) or naphthalene-1,8:4,5-bis(dicarboximide) (ndi), with either propane or xylene group as linkers, have been prepared. The mono- and dinuclear Ru complexes containing the bdi or ndi ligand, exhibit characteristic metal-to-ligand charge transfer (MLCT) transition at 458 nm. The mono- and dinuclear Ru/Os complexes exhibit a rich redox chemistry arising from both M(II) to M(III) oxidation and ligand-based consecutive reduction of diimide and 2,2′-bipyridine (bpy) ligands. The emission decays fit well with double- or triple-exponential decay models. The non-exponential decay curve reveals the existence of several conformers in solution due to the flexible propane or *p*-xylene linker. The much shorter emission lifetimes of the $[M(bpy)_2(L\text{-diimide-L})]$ complexes compared with the parent $[M(bpy)_2L]$ indicates the intramolecular electron-transfer from the excited $M(bpy)_2$ moiety to the diimide. The fastest rates of electron transfer ($3 \cdot 10^{10}$ s^{-1}) are attributable to the folded conformers suitable for the electron donor/acceptor through-space interaction. A time-resolved absorption spectroscopic study of the dinuclear bdi and ndi complexes revealed appearance of the electron-transfer products, M(III) and the diimide radical anion, and their rapid disappearance. The effect of the linkers of the ligand L-diimide-L on the rates of electron transfer and the back electron transfer is also discussed.

Keywords: Electrochemistry; Photochemistry; Ruthenium complexes; Osmium complexes; Photoinduced electron transfer; Diimides; Bipyridines.

Electron transfer reactions play a key role in biological processes such as photosynthesis, and are also at heart of many important chemical processes[1]. The photosynthetic centre uses a multistep electron transfer through a set of donor and acceptor moieties in order to achieve long-range charge separation and to reduce the rapid charge recombination by spatially separating the electron and hole. During the past two decades photoinduced intramolecular electron transfer reactions in dyad, triad and tetrad assemblies have been extensively examined towards mimicking the photosynthetic centre[2–8]. In a triad system, several different molecular sequences for a combination of electron donors (D) and acceptors (A) can be considered. Most studied sequences are D–D*–A and D*–A–A triad systems, in which porphyrin and $[Ru(bpy)_3]^{2+}$ (bpy = 2,2′-bipyridine) are used as chromophores (D) and *p*-quinone and methylviologen as electron acceptors[2–5,9–11]. These two types of molecules can in principle give rise to long-lived, charge-separated states, D^+–D–A^-, as a result of sequential electron transfer reactions provided the redox potentials of the donors and acceptors are judiciously selected. Recently, the diimide units have been used as an electron acceptor in porphyrin triad systems[12,13]. Since the diimide radical anion possesses characteristic intense absorption bands between 600–700 nm, the transient species resulting from the photoinduced electron transfer can be easily detected by transient absorption spectra[14–18]. Furthermore, the naphthalenebis(dicarboximide) is used as DNA-binding molecules or donor–acceptor π-stacked supramolecular host systems[19–23]. So far, several reports on a combination of $[Ru(bpy)_3]^{2+}$ as an electron donor and diimide units as electron acceptors, have been published[20,24]. A novel bridging ligand, L-diimide-L was prepared, in which the diimide unit is linked by two bidentate ligand units (L) such as bpy or 2-(2-pyridyl)-benzimidazole (pbimH). The bpy-diimide-bpy ligand was also used as a building block linker for self-assembling to metallomacrocycles[23]. In the present paper, we describe syntheses of a series of Ru/Os complexes with this novel bridging ligand containing the carboximide group (Scheme 1). Their photoinduced electron transfer reactions were examined and the results are reported hereinafter. A preliminary result for a Ru^{II}-(L-diimide-L)-Os^{III} complex has been reported elsewhere[24].

EXPERIMENTAL

Materials

Acrylonitrile (Nacalai) and ruthenium trichloride trihydrate (Engelhardt) were used without further purification. Acetonitrile was purified twice by distillation over P_2O_5. Tetrabutylammonium tetrafluoroborate ($TBABF_4$, Nacalai) and tetrabutylammonium perchlorate ($TBAClO_4$, Nacalai) were recrystallized from ethanol–water (4 : 1 v/v) and dried *in vacuo*. All other supplied chemicals were of standard reagent grade quality.

The compounds 2-(2-pyridyl)benzimidazole[25], 4,4′-bis(trifluoromethyl)-2,2′-bipyridine (btfmb)[26], $[Ru(bpy)_2Cl_2]\cdot 2H_2O$ (ref.[27]), $[Ru(btfmb)_2Cl_2]\cdot 2H_2O$ (ref.[26]) and $[Os(bpy)_2Cl_2]\cdot 2H_2O$ (ref.[27]) were synthesized according to literature procedures.

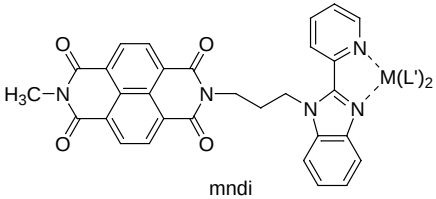

mndi

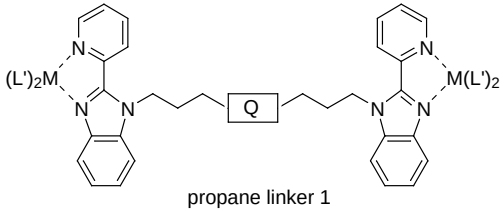

propane linker 1

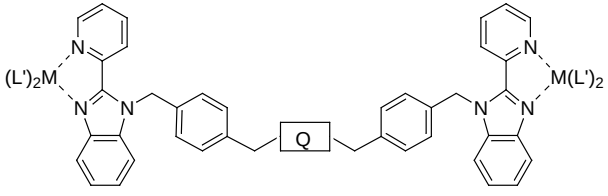

p-xylene linker 2

M = Ru or Os; L' = bpy, dmbpy, btmfb

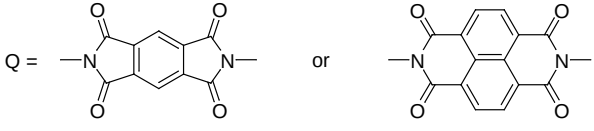

pbdi: linker 1
xbdi: 2

pndi: linker 1
xndi: 2

SCHEME 1

Syntheses of Ligands

1-(Cyanoethyl)-2-(2-pyridyl)benzimidazole (**2**)

2-(2-Pyridyl)benzimidazole (**1**) (8.6 g, 44.1 mmol) was dissolved in warm 1,4-dioxane (120 ml). Next, tetramethylammonium hydroxide in 25% methanol solution (0.5 ml) was added. The light pink colour of the reaction solution disappeared. To the resulting solution acrylonitrile (5.84 g, 0.11 mol) was added dropwise. During the addition the colour turned red and a small amount of precipitate was formed. The solution mixture was heated at 120 °C overnight. After cooling to room temperature, the solution was filtered to remove a red brown precipitate. The filtrate was evaporated *in vacuo*. The resulting oily residue was redissolved in a minimum volume of acetone, followed by the addition of a large volume of ether to precipitate the product. The precipitate was collected and crystallized from methanol–water as white needles. Yield 6.5 g (60%). The product is soluble in common organic solvents. M.p. 105–110 °C. IR (KBr disk): ν(CN) at 2 280 cm^{-1}. ^1H NMR ($CDCl_3$): 3.16 (t, 2 H, J = 3.7); 5.07 (t, 2 H, J = 3.1); 7.34 (t, 1 H, J = 6.1); 7.38 (t, 1 H, J = 3.7); 7.40 (t, 1 H, J = 7.0); 7.49 (d, 1 H, J = 7.6); 7.86 (d, 1 H, J = 3.7); 7.88 (t, 1 H, J = 1.8); 8.48 (d, 1 H, J = 2.1); 8.70 (d, 1 H, J = 3.1). MS (EI), *m/z*: 248 (M^+). For $C_{15}H_{12}N_4$ calculated: 72.56% C, 4.87% H, 22.57% N; found: 72.54% C, 5.09% H, 22.54% N.

1-(3-Aminopropyl)-2-(2-pyridyl)benzimidazole (**3**)

1-(2-Cyanoethyl)-2-(2-pyridyl)benzimidazole (**2**) (6.0 g, 24.2 mmol) was dissolved in methanol (200 ml), followed by addition of solid cobalt(II) chloride hexahydrate (11.1 g, 48.4 mmol) under stirring. To this solution, 1 g of solid sodium borohydride was added each time until the total amount reached 15 g. ***Caution!*** *A vigorous reaction with violent gas evolution occurred upon the addition of $NaBH_4$. The addition of $NaBH_4$ should be carried out with caution*. As a result, the pink solution colour turned black. After complete addition of sodium borohydride the reaction mixture was stirred at room temperature for another 3 h; during this time the solution colour gradually turned light brown. The solution was then acidified by dropwise addition of concentrated HCl and a white precipitate formed. After filtration and drying *in vacuo*, a blue solid product was left. It was dissolved in water and the solution was made alkaline dropwise addition of 25% NH_3 solution. The resulting solution was extracted with chloroform (5 × 80 ml), and the combined chloroform layer was dried over anhydrous $MgSO_4$. A red-brown oily product was obtained after evaporation of chloroform. This product was dissolved in a minimum volume of pure benzene and a large volume of diethyl ether was added to precipitate impurities. After filtration, the pure product was obtained as red oil by evaporation of the solvent. Yield 4.91 g (80.5%). IR: ν(–NH_2) at 3 350 and 3 280 cm^{-1}. ^1H NMR ($CDCl_3$): 1.62 (s, 2 H); 2.08 (t, 2 H); 2.76 (t, 2 H); 4.94 (t, 2 H); 7.32 (t, 1 H); 7.33 (t, 1 H); 7.33 (t, 1 H); 7.52 (d, 1 H); 7.85 (d, 1 H); 7.88 (t, 1 H); 8.43 (d, 1 H); 8.69 (d, 1 H). MS (EI), *m/z*: 253 (M^+). M = $C_{15}H_{16}N_4$.

1-(4-Cyanobenzyl)-2-(2-pyridyl)benzimidazole (**4**)

2-(2-Pyridyl)benzimidazole (**1**) (8.75 g, 44.9 mmol) in dimethylformamide (DMF; 50 ml) was reacted with sodium hydride (1.97 g, 49.3 mmol, 60% dispersion in mineral oil) which was washed under nitrogen with heptane as to remove the mineral oil. A vigorous reaction occurred, accompanied by evolution of H_2 gas. The pale yellow solution colour turned dark

brown on heating at 80 °C for 2 h. After the gas evolution ceased, 4-(bromomethyl)benzonitrile (8.79 g, 44.9 mmol) in 30 ml of DMF was added dropwise and the solution was refluxed for 14 h. After cooling, the solvent was evaporated *in vacuo*. The residue was redissolved in CH_2Cl_2. The solution was filtered to remove insoluble impurities. The filtrate was evaporated *in vacuo* to obtain a brown product that was recrystallized from a methanol–water mixture. Yield 12.7 g (91%). The product is soluble in common organic solvents. M.p. 154–158 °C. IR (KBr disk): ν(CN) at 2 200 cm^{-1}. ^1H NMR ($CDCl_3$): 6.23 (t, 2 H); 7.26 (d, 2 H, *J* = 3.5); 7.29 (d, 2 H, *J* = 2.0); 7.32 (t, 1 H, *J* = 4.0); 7.36 (t, 1 H, *J* = 4.0); 7.54 (d, 1 H); 7.56 (d, 1 H); 7.82 (t, 1 H, *J* =1.5); 7.85 (t, 1 H, *J* = 4.5); 7.87 (d, 1 H, *J* = 2.0); 7.90 (d, 1 H, *J* = 5.4). MS (EI), *m/z*: 309 (M^+). For $C_{20}H_{14}N_4$ calculated: 77.40% C, 4.55% H, 18.05% N; found: 77.55% C, 4.76% H, 7.83% N.

[4-(Aminomethyl)benzyl]-2-(2-pyridyl)benzimidazole (**5**)

1-(4-Cyanobenzyl)-2-(2-pyridyl)benzimidazole (**4**) (6.0 g,19.3 mmol) and $CoCl_2 \cdot 6H_2O$ (9.2 g, 38.6 mmol) were dissolved in methanol with stirring at room temperature. To this solution solid $NaBH_4$ (8 g, 0.2 mol) was added in 0.5 g portions. ***Caution!*** *A vigorous reaction with violent gas evolution occurred upon the addition of $NaBH_4$. The addition of $NaBH_4$ should be carried out with caution*. After complete addition of $NaBH_4$ the reaction mixture was stirred at room temperature for 2 h. At this stage the black solution colour turned light brown. The solution was then acidified with the dropwise addition of concentrated HCl. A white precipitate was removed by filtration. The filtrate was evaporated *in vacuo* to obtain a blue solid. The solid was redissolved in 25% NH_3 (50 ml). The solution was extracted with five 50 ml portions of chloroform. The combined extracts were dried over anhydrous $MgSO_4$ and evaporated to dryness. A red-brown oily residue was again dissolved in benzene and treated with diethylether to precipitate insoluble impurities that were removed by filtration. The filtrate was again evaporated to dryness. A pure product was obtained as a red oil. Yield 4.7 g (77.3%). IR (KBr disk): ν(NH_2) at 3 220 and 3 280 cm^{-1}. ^1H NMR ($CDCl_3$): 1.66 (s, 2 H); 3.79 (t, 2 H); 6.18 (t, 2 H); 7.15 (d, 2 H, *J* = 8.2); 7.17 (d, 2 H, *J* = 4.9); 7.25 (t, 1 H, *J* = 5.9); 7.30 (t, 1 H, *J* = 2.0); 7.32 (d, 1 H, *J* = 3.0); 7.33 (d, 1 H, *J* = 2.0); 7.81 (t, 1 H, *J* = 7.9); 7.86 (t, 1 H, *J* = 1.3); 8.43 (d, 1 H, *J* = 7.9); 8.63 (d, 1 H, *J* = 4.9). MS (EI), *m/z*: 313 (M^+). *M* = $C_{20}H_{18}N_4$.

N-Methyl-*N'*-{3-[2-(2-pyridyl)benzimidazol-1-yl]propyl}naphthalene-1,8:4,5-bis-(dicarboximide) (mndi)

N-{3-[2-(2-Pyridyl)benzimidazol-1-yl]propyl}naphthalene-1,8:4,5-bis(dicarboximide) (0.5 g, 1 mmol) was dissolved in DMF (50 ml) at 120 °C under an nitrogen atmosphere within 1 h. To the resulting solution methylamine (0.03 g, 1 mmol) was added and heating was continued for another 8 h. The solvent was then evaporated *in vacuo*. A brown product was recrystallized from a mixture of chloroform–methanol. Yield 0.41 g (83%). The product was soluble in $CHCl_3$, DMF, DMSO, CH_2Cl_2. M.p. 230–234 °C. ^1H NMR (CD_3CN): 2.43 (t, 2 H, *J* = 7.3); 3.47 (s, 3 H, *J* = 2.0); 4.22 (t, 2 H, *J* = 7.3); 4.96 (t, 2 H, *J* = 7.6); 7.21 (t, 1 H, *J* = 4.6); 7.26 (t, 1 H, *J* = 6.3); 7.30 (t, 1 H, *J* = 7.6); 7.61 (d, 1 H, *J* = 8.9); 7.66 (d, 1 H, *J* = 7.9); 7.83 (t, 1 H, *J* = 5.6); 8.27 (d, 1 H, *J* = 1.0); 8.30 (d, 1 H, *J* = 7.9); 8.64 (s, 4 H, *J* = 4.6). MS (EI), *m/z*: 515 (M^+). For $C_{30}H_{21}N_5O_4 \cdot 0.5H_2O$ calculated: 68.70% C, 4.23% H,13.35% N; found: 69.09% C; 4.33% H,13.40% N.

Syntheses of Bridging Ligands

N,N′-Bis{3-[2-(2-pyridyl)benzimidazol-1-yl]propyl}benzene-1,2:4,5-bis-(dicarboximide) (pbdi)

Pyromellitic dianhydride (**6**) (1.8 g, 8.26 mmol) was dissolved in toluene (150 ml), followed by addition of triethylamine (2 ml). When the solution became clear, 4.16 g (16.5 mmol) of 1-(3-aminopropyl)-2-(2-pyridyl)benzimidazole (**3**) was added to the reaction mixture. The solution colour turned yellow. The reaction mixture was then refluxed at 200 °C for 5 h, while continuously removing water with a water separator. When the volume of water reached to theoretical value, the reaction was stopped and the solvent was evaporated to dryness. The product was obtained as a yellow solid that was dried *in vacuo*. The crude product was then recrystallized from DMF–water (2 : 1). Yield 4.05 g (71.5%). The product is soluble in DMF, DMSO and ethylene glycol. M.p. 268–272 °C. IR: ν(C=O) at 1 765 and 1 708 cm^{-1}. ^1H NMR (DMSO-d_6): 2.21 (t, 4 H); 3.74 (t, 4 H); 4.90 (t, 4 H); 7.26 (t, 2 H, *J* = 7.6); 7.32 (t, 2 H, *J* = 7.3); 7.39 (t, 2 H); 7.71 (d, 2 H, *J* = 7.9); 7.75 (d, 2 H, *J* = 7.6); 7.95 (t, 2 H); 8.17 (s, 2 H); 8.31 (d, 2 H, *J* = 7.9); 8.39 (d, 2 H). MS (EI), *m/z*: 686 (M^+). *M* = $C_{40}H_{30}N_8O_4$. For $C_{40}H_{30}N_8O_4 \cdot 0.5\ H_2O$ calculated: 69.05% C, 4.49% H, 16.11% N; found: 69.04% C, 4.67% H, 15.59% N.

N,N′-Bis{3-[2-(2-pyridyl)benzimidazol-1-yl)]propyl}naphthalene-1,4:5,8-bis-(dicarboximide) (pndi)

A mixture of naphthalene-1,4:5,8-bis(dicarboxanhydride) (**7**) (2.0 g, 7.46 mmol), 1-(3-aminopropyl)-2-(2-pyridyl)benzimidazole (3.76 g, 14.9 mmol) and triethylamine (2 ml) in toluene (150 ml) was heated at 180 °C for 7 h, while removing the water formed. The grey solution colour solution turned light brown. The solvent was removed *in vacuo*. The crude brown product was recrystallized from DMF. Yield 3.70 g (67.3%). The product is soluble in DMF, DMSO and ethylene glycol. M.p. 226–230 °C. IR (KBr disk): ν(C=O) at 1 700 and 1 660 cm^{-1}. ^1H NMR (DSMO-d_6): 2.20 (t, 4 H); 4.15 (t, 4 H); 4.95(t, 4 H); 7.15 (t, 2 H, *J* = 7.3); 7.24 (t, 2 H, *J* = 7.3); 7.31 (t, 2 H, *J* = 4.9); 7.68 (d, 2 H, *J* = 7.9); 7.72 (d, 2 H, *J* = 8.2); 7.91 (t, 2 H, *J* = 7.6); 8.28 (d, 2 H, *J* = 7.9); 8.31 (d, 2 H, *J* = 0.9); 8.60 (s, 4 H). MS (EI), *m/z*: 736 (M^+). *M* = $C_{44}H_{32}N_8O_4$. For $C_{44}H_{32}N_8O_4 \cdot 0.5H_2O$ calculated: 70.86% C, 4.46% H, 15.02% N; found: 70.72% C, 4.51% H, 14.76% N.

N.N′-Bis(4-{[2-(2-pyridyl)benzimidazol-1-yl]methyl}benzyl)naphthalene1,4:5,8-bis-(dicarboximide) (xndi)

Naphthalene-1,4:5,8-bis(dicarboxanhydride) (**7**) (0.94 g, 3.49 mmol) and triethylamine (1.5 ml) were dissolved in toluene (50 ml) at 180 °C under stirring. Next, 1-[4-(aminomethyl)benzyl]-2-(2-pyridyl)benzimidazole (**5**) (2.2 g, 6.99 mmol) was added. The reflux was continued for another 12 h, during which time the grey solution colour turned brown. The solvent was evaporated *in vacuo*. The resulting brown solid was recrystallized from DMF–methanol. Yield 2.2 g (73%). The product is soluble in DMF, DMSO and ethylene glycol. M.p. > 280 °C. IR: ν(C=O) at 1 660 and 1 692 cm^{-1}. ^1H NMR (DSMO-d_6): 5.16 (t, 4 H); 6.17 (t, 4 H); 7.07 (d, 4 H, *J* = 7.9); 7.22 (t, 2 H, *J* = 8.9); 7.25 (t, 2 H, *J* = 6.9); 7.47 (d, 4H; *J* = 7.4); 7.51 (t, 2 H, *J* = 3.5); 7.71 (d, 2 H, *J* = 5.9); 7.74 (d, 2 H, *J* = 3.0); 7.98 (t, 2 H, *J* = 7.9); 8.34 (d, 2 H, *J* = 7.4); 8.61 (s, 4 H); 8.65 (d, 2 H, *J* = 4.9). MS (EI), *m/z*: 860 (M^+). *M* =

$C_{54}H_{36}N_8O_4$. For $C_{54}H_{36}N_8O_4 \cdot H_2O$ calculated: 73.79% C, 4.36% H, 12.75% N; found: 73.77% C, 4.49% H, 12.04% N.

Caution! *Perchlorate salts are potentially explosive. Although no detonation tendencies have been observed, caution is advised and handling of only small quantities is recommended.*

Syntheses of Mononuclear Complexes

$[Ru(bpy)_2(pbdi)](ClO_4)_2 \cdot 3H_2O$

The ligand, pbdi (0.30 g, 0.44 mmol), was dissolved in ethylene glycol (30 ml) by heating. Next, solid $[Ru(bpy)_2Cl_2]$ (0.21 g, 0.44 mmol) was added to the solution. The temperature of 180 °C was maintained for another 5 h. During this time the violet colour of the reaction mixture turned red. After cooling, water (30 ml) was added to the reaction mixture, followed by filtration. To the filtrate, a saturated solution of $NaClO_4$ was added dropwise to complete precipitation. The precipitate was collected and dried *in vacuo*. Its purification was performed by SP-Sephadex C-25 column chromatography, using acetonitrile–buffer (1 : 1) of different pH as an eluent. The desired band was eluted at pH 5.0. Evaporation of acetonitrile from the eluate and addition of a saturated $NaClO_4$ solution afforded a red precipitate that was purifed by recrystallization from methanol. Yield 0.22 g (37%). For $C_{60}H_{46}Cl_2N_{12}O_{12}Ru \cdot 3H_2O$ calculated: 53.26% C, 3.87% H, 12.42% N; found: 53.53% C, 4.12% H, 12.0% N.

$[M(bpy)_2(pndi)](ClO_4)_2 \cdot xH_2O$ (M = Ru, x = 2; M = Os, x = 4)

The synthetic procedure is the same as that used for the corresponding mononuclear pbdi complex. For the Os complex, a longer reflux time was used.

M = Ru, x = 2. Yield 45%. For $C_{64}H_{48}Cl_2N_{12}O_{12}Ru \cdot 2H_2O$ calculated: 55.50% C, 3.78% H, 12.13% N; found: 55.90% C, 4.05% H, 12.11% N.

M = Os, x = 4. Yield 41%. For $C_{64}H_{48}Cl_2N_{12}O_{12}Os \cdot 4H_2O$ calculated: 47.50% C, 4.23% H, 10.39% N; found: 47.61% C, 3.66% H, 10.34% N.

$[Ru(bpy)_2(xndi)](ClO_4)_2 \cdot 7H_2O$

The synthetic procedure is the same as that used for the corresponding mononuclear pndi complex. Yield 0.18 g (35%). For $C_{74}H_{52}Cl_2N_{12}O_{12}Ru \cdot 7H_2O$ calculated: 55.57% C, 4.16% H, 10.51% N; found: 55.65% C, 3.75% H, 10.39% N.

$[Ru(bpy)_2(mndi)](ClO_4)_2.2H_2O$

The mndi ligand (0.20 g, 0.39 mmol) was stirred in 30 ml of ethylene glycol at 180 °C under a nitrogen atmosphere for 1 h. Solid $[Ru(bpy)_2Cl_2]$ (0.19 g, 0.39 mmol) was added to the reaction mixture and heated for another 5 h. During this time the brown solution colour turned red. After cooling to room temperature, water (30 ml) was added and the reaction mixture was filtered. To the filtrate, a saturated $NaClO_4$ solution was added. A red precipitate was collected and dried. The sample was then loaded on a SP-Sephadex C-25 column and eluted with acetonitrile–buffer (1 : 1 v/v), adjusting pH. The desired band was eluted at pH 4.5. The solution was concentrated *in vacuo*. Next, a saturated $NaClO_4$ solution was added to precipitate the desired complex. The precipitate was collected by filtration and

recrystallized from methanol. Yield 0.24 g (55%). For $C_{50}H_{37}Cl_2N_9O_{12}Ru \cdot 2H_2O$ calculated: 51.55% C, 3.52% H, 10.83% N; found: 51.24% C, 2.84% H, 10.73% N.

Syntheses of Dinuclear Complexes

$[\{Ru(bpy)_2\}_2(\mu\text{-pbdi})](ClO_4)_4 \cdot 3H_2O$

A solution of $[Ru(bpy)_2Cl_2]$ (0.17 g, 0.35 mmol) in ethylene glycol (30 ml) was heated at about 180 °C for 30 min. Solid pbdi (0.12 g, 0.17 mmol) was added to the hot solution and the heating was continued for another 8 h. The colour of the solution turned red. After cooling the solution to room temperature, water (30 ml) was added to precipitate unreacted pbdi ligand. After filtration, a saturated aqueous $NaClO_4$ solution was added to complete the precipitation. The red precipitate was collected and dried. The crude product was purified by SP-Sephadex C-25 column chromatography, using acetonitrile–buffer (1 : 1 v/v) eluent. The desired band was eluted at pH 7.0. Further purification was achieved by recrystallization from methanol. Yield 0.30 g (54%). MS (ESI) (CH_3CN), *m/z*: 856 ($[M - 2\ X]^{2+}$), 537 ($[M - 3\ X]^{3+}$), 378 ($[M - 4\ X]^{4+}$). For $C_{80}H_{62}Cl_4N_{16}O_{20}Ru_2 \cdot 3H_2O$ calculated: 48.89% C, 3.49% H, 11.40% N; found: 48.67% C, 3.81% H, 11.20% N.

$[\{M(bpy)_2\}_2(\mu\text{-pndi})](ClO_4)_4 \cdot xH_2O$ (M = Ru, x = 3; M = Os, x = 4)

These complexes were synthesized in a similar manner as $[\{Ru(bpy)_2\}(\mu\text{-pbdi})](ClO_4)_4 \cdot 3H_2O$, except that pndi was used instead of pbdi. Yield 40%.

M = Ru. MS (ESI) (CH_3CN), *m/z*: 881 ($[M - 2\ X]^{2+}$), 554 ($[M - 3\ X]^{3+}$), 391 ($[M - 4\ X]^{4+}$). For $C_{84}H_{64}Cl_4N_{16}O_{20}Ru_2 \cdot 3H_2O$ calculated: 50.06% C, 3.50% H, 11.12% N; found: 49.90% C, 3.73% H, 11.07% N.

M = Os. For $C_{84}H_{64}Cl_4N_{16}O_{20}Os_2 \cdot 4H_2O$ calculated: 45.62% C, 3.28% H, 10.13% N; found: 45.43% C, 3.40% H, 10.06% N.

$[\{RuL'_2\}_2(\mu\text{-pndi})](ClO_4)_4 \cdot xH_2O$ (L′ = dmbpy, x = 7; L′ = btmfb, x = 2)

These complexes were prepared in a similar manner as the corresponding homodinuclear pbdi complex above, except that $[RuL'_2Cl_2]$ (L′ = dmbpy or btmfb) were used as starting complexes. Purification was accomplished by column chromatography using the SP-Sephadex C-25 resin, followed by recrystallization from methanol.

L′ = dmbpy. Yield 0.24 g (50%). For $C_{92}H_{80}Cl_4N_{16}O_{20}Ru_2 \cdot 7H_2O$ calculated: 50.23% C, 4.31% H, 10.19% N; found: 50.36% C, 4.21% H, 10.21% N.

L′ = btmfb. Yield 0.23 g (55.8%). For $C_{92}H_{56}Cl_4F_{24}N_{16}O_{20}Ru_2 \cdot 2H_2O$ calculated: 43.48% C, 2.38% H, 8.82% N; found: 43.55% C, 2.68% H, 8.45% N.

$[Ru(bpy)_2(\mu\text{-pbdi})Os(bpy)_2](ClO_4)_4 \cdot 4H_2O$

$[Ru(bpy)_2Cl_2]$ (0.052 g, 0.11 mmol) in ethylene glycol (30 ml) was heated at 180 °C under a nitrogen atmosphere for 1 h. Next, $[Os(bpy)_2(pbdi)](ClO_4)_2$ (0.15 g, 0.11 mmol) was added to the solution. The heating was continued for another 10 h. The red solution colour turned light green. Water (30 ml) was added to remove the unreacted pbdi ligand. A saturated solution of $NaClO_4$ was added to the filtrate to complete the precipitation. The resulting green precipitate was filtered and dried *in vacuo*. The crude product was purified by chromatogra-

phy on SP-Sephadex C-25 resin, using acetonitrile–buffer (1 : 1 v/v) as eluent. The desired band was eluted at pH 7.0. The light green powder product was recrystallized from methanol. Yield 0.13 g (61%). For $C_{80}H_{62}Cl_4N_{16}O_{20}OsRu \cdot 4H_2O$ calculated: 46.36% C, 3.40% H, 10.81% N; found: 46.89% C, 4.03% H, 10.65% N.

$[Ru(bpy)_2(\mu\text{-pndi})Os(bpy)_2](ClO_4)_4 \cdot 4H_2O$

$[Ru(bpy)_2Cl_2]$ (0.099 g, 0.21 mmol) was dissolved in 30 ml of ethylene glycol at 180 °C under a nitrogen atmosphere while stirring for 1 h. Next, $[Os(bpy)_2(pndi)]^{2+}$ (0.30 g, 0.21 mmol) was added and heating was continued for another 12 h, during which time the red solution colour turned light green. After being cooled to room temperature, 30 ml of water was added and the solution was filtered. A saturated aqueous solution of $NaClO_4$ was added dropwise to the filtrate to complete the precipitation. A light green precipitate was collected and purified by column chromatography on SP-Sephadex C-25 resin, using acetonitrile–buffer (1 : 1 v/v) as eluent. The desired band was eluted at pH 7.0. The volume of the collected eluate was reduced to the half and $NaClO_4$ was added to complete the precipitation. The precipitate was collected and recrystallized from methanol. Yield 0.26 g (62%). MS (ESI) (CH_3CN), *m/z*: 926 ($[M - 2\ X]^{2+}$), 584 ($[M - 3\ X]^{3+}$), 413 ($[M - 4\ X]^{4+}$). For $C_{84}H_{64}Cl_4N_{16}O_{20}OsRu \cdot 4H_2O$ calculated: 47.53% C, 3.42% H, 10.56% N; found: 47.50% C, 3.84% H, 10.42% N.

$[\{Ru(bpy)_2\}_2(\mu\text{-xndi})](ClO_4)_4 \cdot 5H_2O$

The synthetic procedure was the same as that used for the dinuclear pndi analogue, substituting pndi for xndi. Yield 0.34 g (61%). For $C_{94}H_{680}Cl_4N_{16}O_2Ru_2 \cdot 5H_2O$ calculated: 51.89% C, 3.6% H, 10.30% N; found: 51.90% C, 3.48% H, 10.31% N.

$[Ru(bpy)_2(\mu\text{-xndi})Os(bpy)_2](ClO_4)_4 \cdot 10H_2O$

$[Os(bpy)_2Cl_2]$ (0.06 g, 0.1 mmol) was dissolved in ethylene glycol (30 ml) at 180 °C under a nitrogen atmosphere while stirring for 1 h. Next, the solid, $[Ru(bpy)_2(xndi)]^{2+}$ (0.15 g, 0.1 mmol), was added and heating was continued for another 10 h, during which time the black solution colour turned light green. Upon cooling, 30 ml of water was added to remove excess uncoordinated ligand. To the filtrate a saturated $NaClO_4$ solution was added. The resulting precipitate was collected and dried *in vacuo*. Purification was done by SP-Sephadex C-25 column chromatography, using acetonitrile–buffer (1 : 1 v/v) as an eluent. The eluted band at pH 7.0 was collected and the eluate volume reduced to the half by removal of acetonitrile. To the concentrated solution, a saturated solution of $NaClO_4$ was added. The resulting red-green precipitate was collected and recrystallized from methanol. Yield 0.09 g (41%). For $C_{94}H_{68}Cl_4N_{16}O_{20}OsRu \cdot 10H_2O$ calculated: 47.94% C, 3.77% H, 9.52% N; found: 47.54% C, 3.35% H, 9.24% N.

Physical Measurements

Electronic absorption spectra were recorded on a Hitachi U-3210 spectrophotometer (200–850 nm) and a Hitachi U-3400 spectrophotometer (800–2 500 nm). NMR spectra were measured with a 270 MHz JEOL JNM-EX spectrometer. Chemical shifts are given in ppm (δ-scale), coupling constants, *J*, in Hz. IR spectra were recorded on a Nicolet FT-IR Magna

560 spectrometer. The mass spectra were measured on a Shimadzu QP1000EX spectrometer for organic ligands, and on Finnigan–Matt TSQ-700 triple quadrupole mass spectrometer, equipped with ESI interface system, for the complexes.

Electrochemical measurements were made at 20 °C with a BAS 100 B/W electrochemical workstation. The working electrode was a BAS glassy carbon (3-mm diameter) or BAS platinum (1.6-mm diameter) disk. The auxiliary electrode was a platinum wire. The reference electrode was $Ag/AgNO_3$ (10^{-2} M solution in 10^{-1} M $TBABF_4/CH_3CN$). The ferrocene/ferrocenium (Fc/Fc^+) couple was used as an internal reference standard; all potentials in this work are reported *vs* Fc/Fc^+. The value $E_{1/2}(Fc/Fc^+)$ was +0.09 V *vs* Ag/Ag^+ and +0.43 V *vs* SCE. *In situ* UV-VIS spectroelectrochemistry was performed by using a platinum minigrid (80 mesh) working electrode in a thin-layer cell (optical path of 0.05 cm) as described elsewhere[28]. For the generation of Ru^{II}-ndi-Os^{III} mixed-valent complexes in the course of the transient absorption spectral measurement, a flow-through electrolytic method was used as previously described[29]. The quantitative oxidative electrolysis of Ru^{II}-ndi-Os^{II} complex was performed at +0.5 V in acetonitrile solution containing 10^{-1} M $TBAClO_4$.

A Hitachi spectrofluorimeter, Model MPF-2A, was used to measure emission spectra at room temperature. Emission lifetimes were determined by means of the time-correlated single-photon-counting system[30]. A deaerated sample solution in 2-mm quartz cell was excited with the second harmonics of a cavity-dumped Ti^{3+}: Sapphire laser (400 nm, 1 nJ/pulse, 2 kHz–76 MHz) or a LD-excited solid-state laser (532 nm, 1 μJ/pulse, 10 kHz, Nanolase). The typical full width at half maximum (fwhm) of instrumental response function using the former laser is 40 ps and 1 ns for the latter. Transient absorption spectra were obtained after exposure of a sample solution in quartz cell of 2 mm optical length to the second harmonic pulse of the mode-locked Nd^{3+}-YAG laser (2–7 mJ/pulse, fwhm = 17 ps, 10 Hz, PY61C-10 Continuum). The details of the measurement system were reported elsewhere[31]. Time-resolved difference absorption spectra in a delay time range of 0–6 000 ps were measured using the system. Excitation pulses of adequate energy were selected by using a PIN photodiode energy monitor. A white-light pulse was produced by focusing the fundamental-oscillation light into flowing H_2O–D_2O (1 : 1 v/v). The pulse delay was tuned using an optical delay with a movable mirror. The time origin of the white-light pulse was assigned to a time when the absorbance change due to a primary photoproduct was one-half of its maximum value. Two sets consisting of an imaging spectrograph with 150 grooves/mm (Chromex 250IS) and an air-cooled MOS-type linear image sensor with 512 elements (Hamamatsu S4805-512), were used for the detection of monitoring light in front of and behind a sample cell of 1–10 mm optical length. Signals of the image sensor were digitized and fed to a computer, thereby having selected monitoring pulses of adequate intensity. The dark signals without monitoring the light pulse were averaged over 200 measurements, with and without laser excitation.

RESULTS AND DISCUSSION

Preparation of Ligands and Complexes

We succeeded to functionalize 2-(2-pyridyl)benzimidazole (pbimH) to obtain a bridging ligand[32–35] by substituting the imino NH group in pbimH with 2-cyanoethyl and 3-aminopropyl groups (Scheme 2). This allowed us

to synthesize a wide variety of ligands with electron acceptor/donor or additional coordination sites. 1-(3-Aminopropyl)- (**3**) and [4-(aminomethyl)benzyl]-2-(2-pyridyl)benzimidazole (**5**) are good precursors of extended multifunctional ligands or labelling reagents in biomolecules. Novel bis(bidentate) ligands containing diimide as an electron acceptor were obtained by the condensation reaction of an amino derivative of benzimidazole and a tetracarboxylic dianhydride in toluene. The ligands are well soluble in polar solvents such as DMF and DMSO and sparingly soluble in ethylene glycol and alcohol. Mononuclear Ru or Os complexes were synthesized from the reaction of the ligand with one molar equivalent of $[Ru(bpy)_2Cl_2]\cdot 2H_2O$ or $[Os(bpy)_2Cl_2]\cdot 2H_2O$ in ethylene glycol. However, the product was always contaminated with a small amount of dinuclear complex that was carefully separated by SP-Sephadex cation-exchange chromatography. Homodinuclear Ru complexes were obtained by the reaction of the ligand with two molar equivalents of $[RuL'_2Cl_2]\cdot 2H_2O$ (L′ = 2,2′-bipyridine (bpy), 4,4′-dimethyl-bpy (dmbpy), 4,4′-bis(trifluoromethyl)-bpy (btmfb)). Furthermore, the reaction of $[Ru(bpy)_2Cl_2]$ with one molar equivalent of a mononuclear Os complex, $[Os(bpy)_2L]^{2+}$ produced the corresponding heterodinuclear Ru-L-Os complex. The composition of these complexes was established with electrospray mass spectroscopy, NMR and elemental analyses.

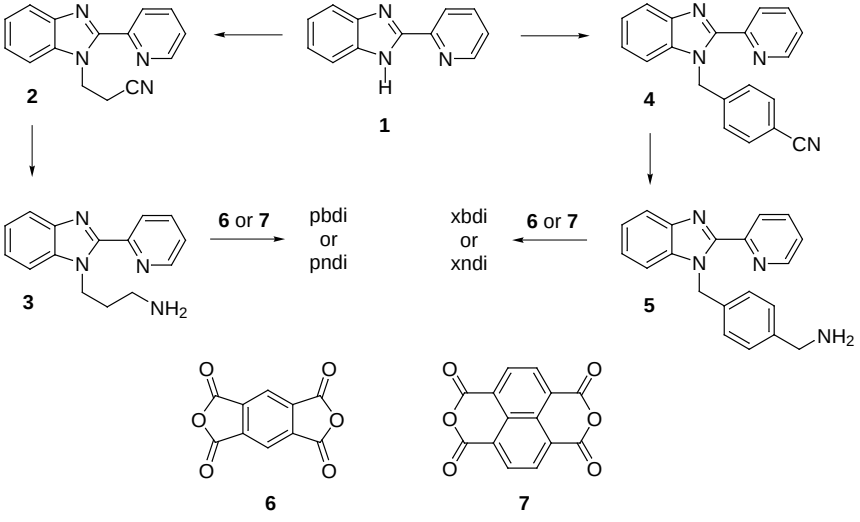

SCHEME 2

Absorption Spectra

The spectral data are summarized in Table I. The novel ligands show π–π* absorption at 312 nm for pbdi, and at 381, 360 and 312 nm for pndi[36]. The mononuclear and dinuclear Ru(II) and Os(II) complexes containing the diimide ligand possess metal-to-ligand (bpy) charge transfer (MLCT) band at 458 nm (for Ru) and 620 nm (for Os), in addition to ligand π–π* bands. The energy of the MLCT transition remains unaltered when the bridging ligand is changed from pbdi to pndi. The UV-VIS spectrum of the mixed-metal RuOs dinuclear complex, $[Ru^{II}(bpy)_2(\mu\text{-pndi})Os^{II}(bpy)_2]^{4+}$, is essentially the sum of the spectra of the components. This complex shows intraligand π–π* transitions of pndi at 322 and 378 nm.

Redox Properties of the Complexes

Redox potentials of the investigated complexes are collected in Table II. All the studied Ru(bpy) complexes show only one reversible Ru(II)/Ru(III) anodic wave at +0.78 ± 0.02 V *vs* Fc/Fc^+, regardless the diimide group and the nuclearity of the complex. Coulometry of the dinuclear complexes revealed that the oxidation involves two electrons. Thus, the potential difference between the two unresolved one-electron steps is the statistical minimum of 40 mV (K_c = 4), judging from the peak-to-peak separation in the cyclic voltammogram by using the simulated curve reported by Richardson and Taube[37]. These results suggest negligible interaction between the two Ru centres. The reduction processes are strongly dependent on the diimide group in the complexes. Mononuclear $[Ru(bpy)_2(pbdi)]^{2+}$ shows three reversible one-electron cathodic waves in CH_3CN; the pyromellitimide group is reduced first, followed by reduction of each bpy ligand. On the other hand, dinuclear $[\{Ru(bpy)_2\}_2(\mu\text{-pbdi})]^{4+}$ exhibits only two two-electron cathodic waves that can be assigned to bpy-localized reduction by comparison of the reduction potentials with those for mononuclear pbdi derivatives. Hence, the two bpy pairs are reduced independently in two 1e + 1e steps due to the lack of electronic communication between the Ru centres. The pyromellitimide reduction is not observed for the dinuclear complex since the pyromellitimide group is covered by the molecular surface of the $Ru(bpy)_2$ moieties, thereby preventing a direct electron transfer from the cathode to the pyromellitimide moiety. Figure 1 shows a cyclic voltammogram of $[\{Ru(bpy)_2\}_2(\mu\text{-pndi})]^{4+}$ in CH_3CN at room temperature. The pndi complex exhibits five reduction processes, the first two being diimide-localized, and the rest bpy-localized. The large cathodic peak for

TABLE I
Absorption and emission data for Ru/Os complexes in CH_3CN at room temperature

Complex	Absorption maxima (ε), nm (M^{-1} cm^{-1})			Emission maximum, nm
	bpy(π–π*)	BL(π–π*)	MLCT(d_π–π*)	
Mononuclear				
$[Ru(bpy)_2(pbdi)]^{2+}$	289 (74 000)	–	458 (14 000)	640
$[Ru(bpy)_2(mndi)]^{2+}$	289 (76 900)	376 (31 700) 355 (32 000) 337 (34 300) 320 (36 100)	458 (17 100)	[a]
$[Ru(bpy)_2(pndi)]^{2+}$	289 (99 000)	378 (38 500) 357 (36 500)	457 (18 000)	[a]
$[Ru(bpy)_2(xndi)]^{2+}$	287 (82 000)	379 (32 900) 358 (30 500)	459 (15 800)	650
$[Os(bpy)_2(pbdi)]^{2+}$	292 (88 200)	453 (14 200)	602 (4 000) 487 (15 600)	[a]
$[Os(bpy)_2(pndi)]^{2+}$	292 (90 000)	378 (38 000) 357 (33 000)	626 (4 100) 484 (15 000)	[a]
Dinuclear				
$[\{Ru(bpy)_2\}_2(\mu\text{-pbdi})]^{4+}$	289 (130 000)	–	458 (28 200)	642
$[\{Ru(bpy)_2\}_2(\mu\text{-pndi})]^{4+}$	289 (159 000)	378 (45 400) 320 (68 500)	459 (35 600)	[a]
$[\{Ru(bpy)_2\}_2(\mu\text{-xndi})]^{4+}$	289 (144 900)	379 (40 900) 320 (60 600)	459 (32 800)	660
$[\{Os(bpy)_2\}_2(\mu\text{-pndi})]^{4+}$	292 (133 000)	378 (42 000) 321 (51 000)	617 (7 000) 486 (26 000)	[a]
$[\{Ru(dmbpy)_2\}_2(\mu\text{-pndi})]^{4+}$	288 (138 200)	378 (39 900) 356 (40 400) 321 (61 600)	464 (31 300)	[a]
$[\{Ru(btfmb)_2\}_2(\mu\text{-pndi})]^{4+}$	290 (153 500)	378 (44 200) 340 (55 700)	478 (25 100)	688
$[Ru(bpy)_2(\mu\text{-pbdi})Os(bpy)_2]^{4+}$	291 (128 600)	–	610 (3 458) 459 (25 760)	[a]
$[Ru(bpy)_2(\mu\text{-pndi})Os(bpy)_2]^{4+}$	290 (147 000)	378 (45 000) 322 (60 000)	620 (3 900) 457 (29 500)	[a]
$[Ru(bpy)_2(\mu\text{-xndi})Os(bpy)_2]^{4+}$	290 (152 100)	379 (47 100) 357 (44 000) 322 (62 000)	605 (4 300) 458 (31 200)	654

[a] Not detected at room temperature.

the 4th reduction process in Fig. 1, labelled with an asterisk, arises from adsorption of reduction products onto the electrode surface.

Varying the substituents R on the bpy ligand in $[\{RuL'_2\}_2(\mu\text{-pndi})]^{4+}$ (R = H, L′ = bpy; R = CH_3, L′ = dmbpy; R = CF_3, L′ = btmfb), the oxidation potential is shifted in the positive direction in the order of R = H < CH_3 < CF_3; although, the first reduction potential remains almost unaltered, indicating the pndi reduction.

TABLE II
Electrochemical data for Ru/Os complexes in CH_3CN containing 10^{-1} M TBAB as a supporting electrolyte

Complex	Oxidation[a]		Reduction[a]	
	Os(II/III)	Ru(II/III)	Diimide$^{0/n-}$	bpy$^{0/-}$
Mononuclear				
$[Ru(bpy)_2(pbdi)]^{2+}$		+0.79	–1.18	–1.79, –1.98
$[Ru(bpy)_2(mndi)]^{2+}$		+0.77	–0.95, –1.34	–1.78, –1.98
$[Ru(bpy)_2(pndi)]^{2+}$		+0.78	–0.93, –1.34	–1.79, –1.97
$[Ru(bpy)_2(xndi)]^{2+}$		+0.78	–0.93, –1.31	–1.74, –1.98
$[Os(bpy)_2(pbdi)]^{2+}$	+0.36		–1.18	–1.67, –1.95
$[Os(bpy)_2(pndi)]^{2+}$	+0.36		–0.94, –1.35	–1.73, –1.92
Dinuclear				
$[\{Ru(bpy)_2\}_2(\mu\text{-pbdi})]^{4+}$		+0.76		–1.74, –2.08
$[\{Ru(bpy)_2\}_2(\mu\text{-pndi})]^{4+}$		+0.78	–0.91, –1.30	–1.76, –1.98
$[\{Ru(bpy)_2\}_2(\mu\text{-xndi})]^{4+}$		+0.78	–0.92, –1.32	–1.72, –1.99
$[\{Os(bpy)_2\}_2(\mu\text{-pndi})]^{4+}$	+0.36		–0.91, –1.29	–1.67, –1.93
$[\{Ru(dmbpy)_2\}_2(\mu\text{-pndi})]^{4+}$		+0.67	–0.91, –1.30	–1.84, –2.03
$[\{Ru(btfmb)_2\}_2(\mu\text{-pndi})]^{4+}$		+1.04	–0.90, –1.31	–1.52, –2.04
$[Ru(bpy)_2(\mu\text{-pbdi})Os(bpy)_2]^{4+}$	+0.33	+0.75		–1.72, –1.99
$[Ru(bpy)_2(\mu\text{-pndi})Os(bpy)_2]^{4+}$	+0.37	+0.79	–0.91, –1.28	–1.73, –1.95
$[Ru(bpy)_2(\mu\text{-xndi})Os(bpy)_2]^{4+}$	+0.36	+0.78	–0.91, –1.31	–1.67, –1.97

[a] $E_{1/2}$, in V *vs* Fc/Fc^+.

Oxidative spectroelectrochemistry of $[\{Ru(bpy)_2\}_2(\mu\text{-pndi})]^{4+}$ at +0.95 V *vs* Fc/Fc^+ shows disappearance of the structured MLCT band at 478 nm and appearance of the bpy π–π* intraligand band at 317 nm, which indicates the formation of the Ru(III) state (Fig. 2a). Similar spectral change has also been observed during the oxidation of $[\{Ru(bpy)_2\}_2(\mu\text{-pbdi})]^{4+}$. On the other hand, the reductive spectroelectrochemistry at –1.1 V *vs* Fc/Fc^+ results in appearance of new bands at 608, 682 and 756 nm that agree with the reported UV-VIS absorption data of the pndi radical anion[15] (Fig. 2b). This result strongly indicates that the first reduction is localized on the bridging pndi moiety. Since no reduction wave for the bdi moiety was observed, the reductive spectroelectrochemistry could not be performed in the latter case.

Cyclic voltammogram of $[Ru^{II}(bpy)_2(\mu\text{-pndi})Os^{II}(bpy)_2]^{4+}$ in CH_3CN shows two anodic processes at +0.37 and +0.79 V and four cathodic processes at –0.91, –1.28, –1.73 and –1.95 V *vs* Fc/Fc^+ (Fig. 3). Comparing the oxidation potentials with those for the corresponding Ru and Os complexes, the oxidation occurs first at the Os site, and then at the Ru site. The potential difference between Ru(II)/Ru(III) and Os(II)/Os(III) oxidations is 0.41 V for the studied dinuclear Ru-Os complex. The first two reductions occur at the naphthalene diimide moiety as sequential one-electron processes, followed by the consecutive bpy-localized one-electron reduction steps.

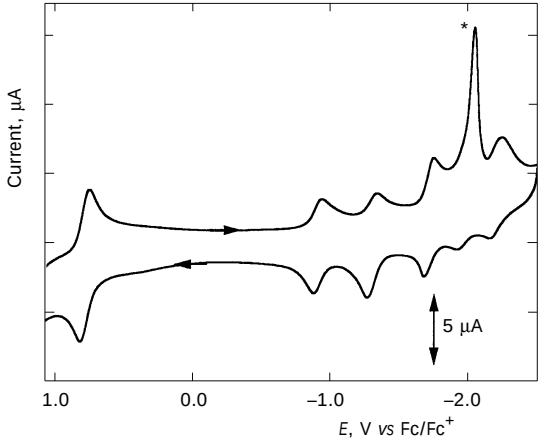

FIG. 1
Cyclic voltammogram of $[\{Ru(bpy)_2\}_2(\mu\text{-pndi})]^{4+}$ in CH_3CN at glassy carbon working electrode at room temperature. The asterisk indicates adsorption at the electrode surface

Figure 4 shows the oxidative spectroelectrochemistry of $[Ru^{II}(bpy)_2(\mu\text{-pndi})Os^{II}(bpy)_2]^{4+}$ in CH_3CN. For the consecutive one-electron oxidations at +0.50 and +0.95 V, the intensities of the MLCT bands at 457 and 620 nm gradually decrease; then, at +0.95 V, complete disappeareance of Ru(II)-to-bpy MLCT band at 459 nm and appearance of new band near 700 nm originating from bpy-to-Ru(III) LMCT transition, were observed. For the first reduction at –1.1 V *vs* Fc/Fc^+, new bands appear at 608, 682 and 756 nm, in addition to increased absorbance at 471 nm, which strongly indicates the formation of ndi radical anion[15] (Fig. 5).

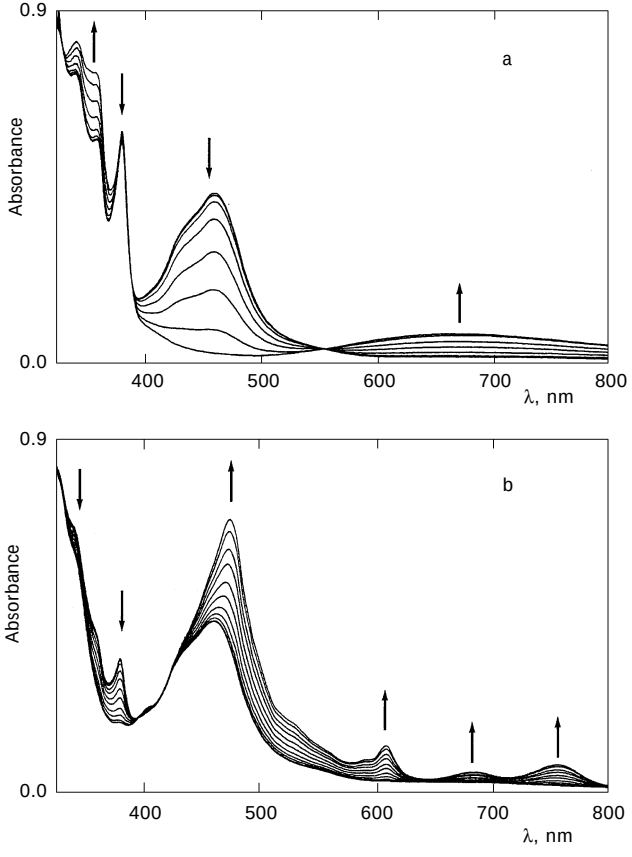

FIG. 2
UV-VIS spectroelectrochemical response of $1 \cdot 10^{-4}$ M $[\{Ru(bpy)_2\}_2(\mu\text{-pndi})]^{4+}$: a oxidation at +0.95 V, b reduction at –1.1 V *vs* Fc/Fc^+

General Aspects of Emission Decays and Transient Absorption Spectra

The parent complexes, $[M(bpy)_2L]$ (L = 2-(2-pyridyl)benzimidazole)) and $[M(bpy)_2(L\text{-}L)]$ (L-L = bis[2-(2-pyridyl)benzimidazole]), show emission at 640–750 nm arising from M-to-bpy CT state[29,33,38] (M = Ru or Os). However, half-lives of emission of the studied $[M(bpy)_2(L\text{-diimide-L})]$ complexes are in general tremendously short compared with those for the parent $[M(bpy)_2(L\text{-}L)]^{2+}$ (660 ns for M = Ru and 34 ns for M = Os)[39] in general. The short emission half-lifes of the studied pbdi, xndi or pndi complexes indicate that electron transfer occurs between the excited $M(bpy)_2$ moiety and diimide. As shown for $[\{Ru(bpy)_2\}_2(\mu\text{-pndi})]^{4+}$ and $[\{Ru(btfmb)_2\}_2(\mu\text{-pndi})]^{4+}$ in Fig. 6, the emission decays, $i(t)$, fit well with a multi-exponential decay model below (Eq. (*1*)),

$$i(t) = A_1 \exp(-t / \tau_1) + A_2 \exp(t / \tau_2) + A_3 \exp(-t / \tau_3), \quad (\tau_1 < \tau_2 < \tau_3) \qquad (1)$$

where A_i and τ_i are the fraction and the lifetime of the decay component (i = 1, 2, 3). The fractions of the third components are only 3–8%, except for $[Ru(bpy)_2(pndi)]^{2+}$, if any. Table III summarizes the determined emission lifetimes for the Ru/Os complexes under study. Since several conformational isomers are present in solution for a propane-linked compound, the

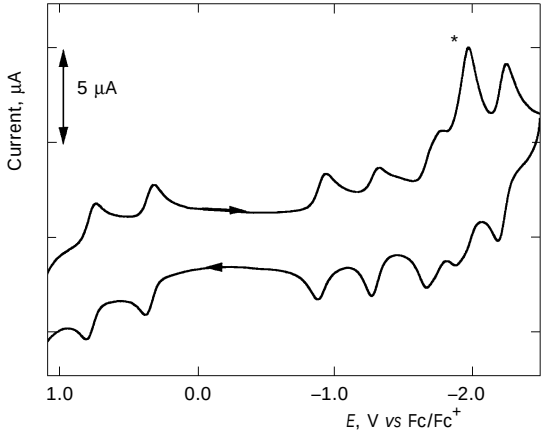

FIG. 3
Cyclic voltammogram of $[Ru^{II}(bpy)_2(\mu\text{-pndi})Os^{II}(bpy)_2]^{4+}$ in CH_3CN at glassy carbon working electrode. The asterisk indicates adsorption at the electrode surface

multi-component decay of emission is interpreted in terms of the conformation isomerism in the propane chain linking. The first components can be assigned to the conformers in which the distance between the electron-donating $Ru(bpy)_2$ and the electron-accepting diimide is sufficiently short to undergo through-space interaction. The slower-decay components are attributable to a common and weak through-bond interaction between the electron-donating $Ru(bpy)_2$ and the electron-accepting diimide for all conformers. Transient absorption spectra recorded during the picosecond laser photolysis have ascertained that quenching the emission bleached the MLCT band. At the same time a new absorption band rised at 715 nm due

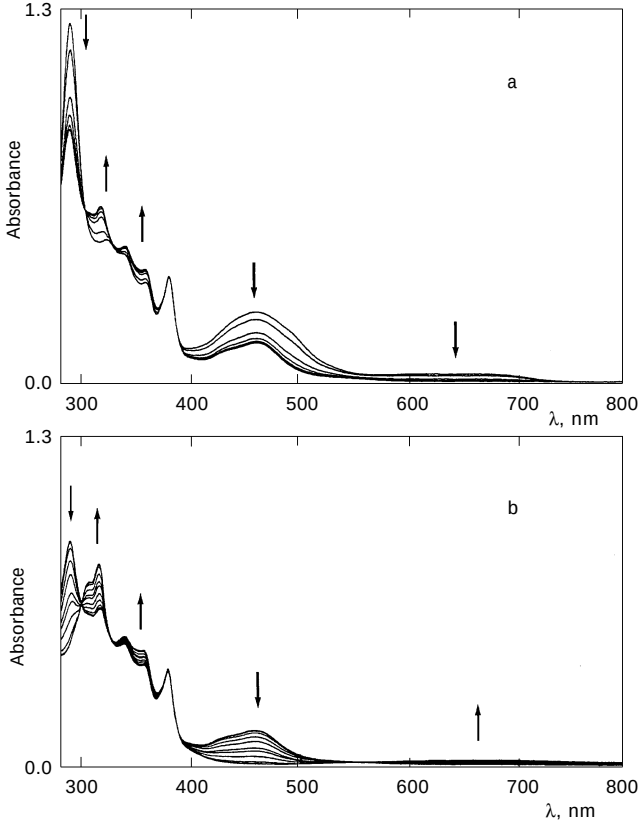

FIG. 4

Oxidative UV-VIS spectroelectrochemistry of $2 \cdot 10^{-4}$ M $[Ru^{II}(bpy)_2(\mu\text{-pndi})Os^{II}(bpy)_2]^{4+}$ at +0.5 and +0.95 V *vs* Fc/Fc^+ in CH_3CN: a first oxidation, b second oxidation

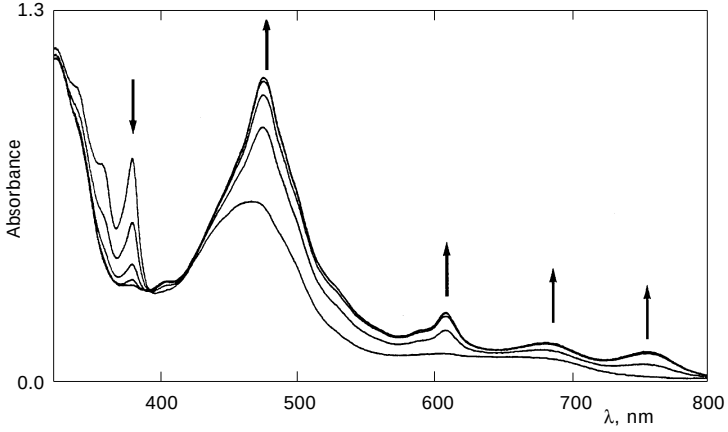

FIG. 5
Reductive UV-VIS spectroelectrochemistry of $2 \cdot 10^{-4}$ M $[Ru^{II}(bpy)_2(\mu\text{-pndi})Os^{II}(bpy)_2]^{4+}$ at –1.1 V *vs* Fc/Fc^+ in CH_3CN

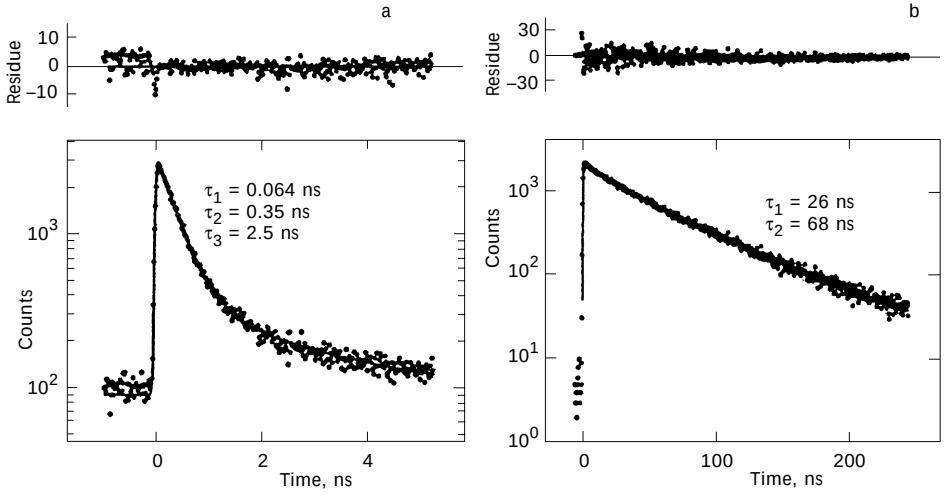

FIG. 6
Typical decay curves for $[\{Ru(bpy)_2\}_2(\mu\text{-pndi})]^{4+}$ (a) and $[\{Ru(btfmb)_2\}_2(\mu\text{-pndi})]^{4+}$ (b), both recorded at 630 nm in CH_3CN at room temperature. Excitation wavelength 400 nm (a) and 532 nm (b)

TABLE III
Emission lifetimes (CH_3CN, room temperature) calculated by multi-exponential decay model

Complex	λ_{excit} [a]	$\lambda_{monitored}$	Emission lifetime[b] (fraction of amplitude)		
			τ_1, ns	τ_2, ns	τ_3, ns
Mononuclear					
$[Ru(bpy)_2(pndi)]^{2+}$	A	630	0.064 (0.55)	0.46 (0.23)	>2.8 (0.2)
$[Ru(bpy)_2(mndi)]^{2+}$	A	630	0.055 (0.47)	0.48 (0.45)	4.4 (0.08)
$[Ru(bpy)_2(pndi)]^{2+}$	A	630	0.082 (0.49)	0.48 (0.37)	3.0 (0.14)
$[Os(bpy)_2(pndi)]^{2+}$	A	730	0.070 (0.62)	0.40 (0.35)	
Dinuclear					
$[\{Ru(bpy)_2\}_2(\mu\text{-pbdi})]^{4+}$	A	630	0.17 (0.21)	3.4 (0.67)	325 (0.12)
$[\{Ru(bpy)_2\}_2(\mu\text{-pndi})]^{4+}$	A	630	0.064 (0.58)	0.35 (0.38)	2.5 (0.04)
$[\{Ru(bpy)_2\}_2(\mu\text{-xndi})]^{4+}$	B	630	6.4 (0.92)	27 (0.08)	
$[\{Os(bpy)_2\}_2(\mu\text{-pndi})]^{4+}$	A	750	0.12 (0.70)	0.47 (0.30)	2.8 (0.03)
$[\{Ru(dmbpy)_2\}_2(\mu\text{-pndi})]^{4+}$	A	630	0.060 (0.69)	0.32 (0.28)	4.0 (0.03)
$[\{Ru(btfmb)_2\}_2(\mu\text{-pndi})]^{4+}$	B	630	26 (0.60)	68 (0.40)	
$[Ru(bpy)_2(\mu\text{-pbdi})Os(bpy)_2]^{4+}$	A	630	26 (0.94)	175 (0.06)	2.4 (0.03)
	A	730	32 (1.00)		
$[Ru(bpy)_2(\mu\text{-pndi})Os(bpy)_2]^{4+}$	A	650	0.060 (0.49)	0.33 (0.47)	
	A	750	0.12 (0.57)	0.42 (0.43)	4.9 (0.04)
$[Ru(bpy)_2(\mu\text{-pndi})Os(bpy)_2]^{5+}$	A	640	0.043 (0.67)	0.35 (0.30)	
$[Ru(bpy)_2(\mu\text{-xndi})Os(bpy)_2]^{5+}$	A	630	64 (0.33)	197 (0.67)	
$[Ru(bpy)_2(\mu\text{-xndi})Os(bpy)_2]^{4+}$	B	620	1.8 (0.44)	6.3 (0.56)	
	B	750	2.2 (0.95)	8.3 (0.05)	
$[Ru(bpy)_2(\mu\text{-xndi})Os(bpy)_2]^{5+}$	B	630	1.4 (0.58)	5.3 (0.42)	

[a] Excitation wavelength; A = 400 nm , B = 532 nm. [b] The values in parentheses show the fraction of emission intensity.

to the radical anion of bdi[15] (Fig. 7), or new bands at 470, 610, 682 and 756 nm due to the radical anion of ndi[15] (Fig. 8).

A similar triple-exponential decay was observed for mononuclear $[Ru(bpy)_2L]^{2+}$ (L = *N*-[3-(2,2′-bipyridine-5-carboxamide)propyl]-*N*′-[3-(dimethylamino)propyl]naphthalene-1,4:5,8-bis(dicarboximide)), the first component of which was proposed to arise from some interaction between the hydrophobic groups of an electron-donating ligand, bpy-5-dicarboxamide, and favourably oriented and located electron-acceptor ndi[20].

The studied propane-linked Ru-diimide complexes also possess conformational isomers, as shown in Scheme 3. Since the through-bond interaction is similar for all the conformers, the rate of electron transfer may not be discriminated. A through-space exchange interaction, such as charge-transfer interaction between the diimide and Ru(bpy) moieties, would increase the fraction of the folded conformers (e and f). Meanwhile, a through-space interaction could not enhance the electron transfer rate up to 10^{10} s^{-1} for the extended conformers (a, b, c and d). Recently, both intramolecular and intermolecular stacking between an ndi and Ru(bpy) moieties was reported for the binuclear Ru compound with aliphatic side

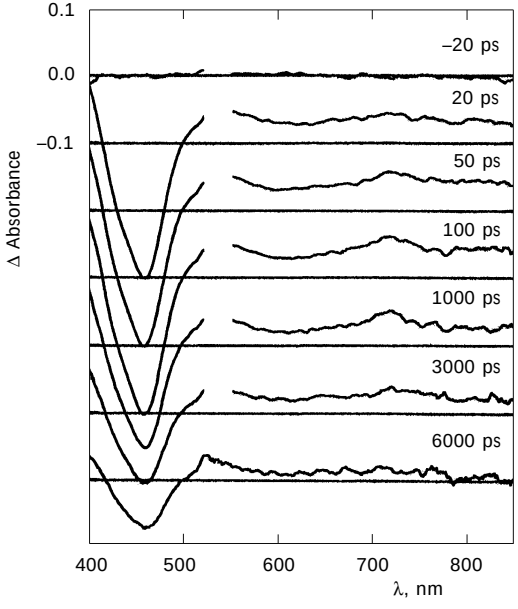

FIG. 7

Picosecond transient difference absorption spectra of $[\{Ru(bpy)_2\}_2(\mu\text{-pbdi})]^{4+}$ in BuCN, following laser pulse excitation (532 nm) of 20 ps duration

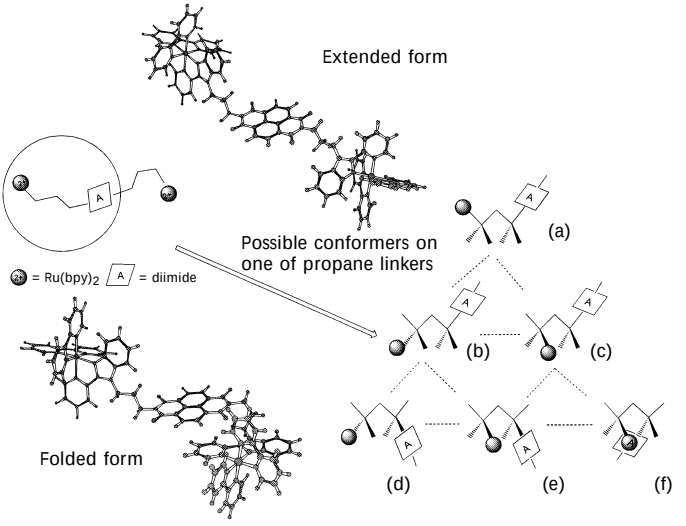

SCHEME 3

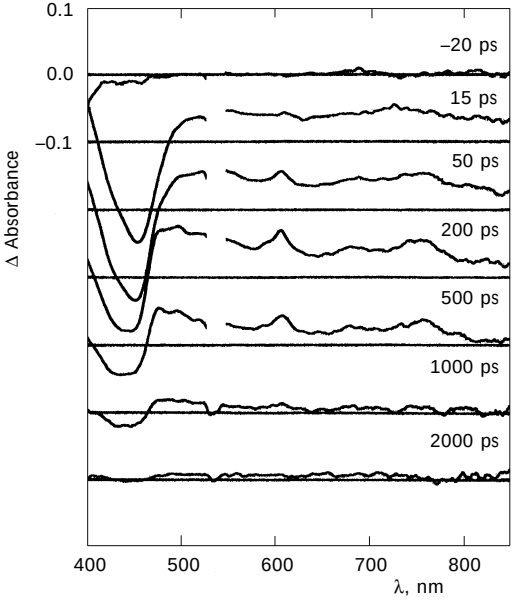

FIG. 8
Picosecond transient difference absorption spectra of $[\{Ru(bpy)_2\}_2(\mu\text{-pndi})]^{4+}$ in BuCN

chain-linker, revealed by ^{1}H NMR spectroscopy[19]. In order to examine the possibility of intramolecular interaction between aromatic rings, the temperature-dependent ^{1}H NMR spectra of $[Ru^{II}(bpy)_2(\mu\text{-pndi})Os^{II}(bpy)_2]^{4+}$ were measured in DMF-d_7. The ^{1}H NMR signals of methylene protons of the imino group of ndi and benzimidazole moiety were observed at δ 4.25 and 5.23, respectively. The former signals were broad and remained unchaged on temperature variation. On the other hand, the latter proton signals of the methylene groups bound to 2-(2-pyridyl)benzimidazole moiety, exhibit temperature dependence. The two components of the broad signal at room temperature coalesced into broad unresolved signal at –50 °C. This result shows the presence of conformers in solution and the dynamic movement of the propane side arm in addition to the restricted rotation about the N–C bond of naphthalenediimide.

Photoinduced Electron-Transfer and Back Electron-Transfer Processes in Dyad Complexes

$[\{Ru(bpy)_2\}_2(\mu\text{-pbdi})]^{4+}$

From the viewpoint of driving force, the photoinduced electron transfer from the excited $Ru(bpy)_2$ moiety to pbdi is feasible (Scheme 4). Figure 7 shows the picosecond transient spectra of $[\{Ru(bpy)_2\}_2(\mu\text{-pbdi})]^{4+}$ in BuCN, recorded after laser pulse excitation (532 nm). This absorption band is characteristic of the anion radical of bdi[15], though it is somewhat broader. The appearance of this band indicates that the anion radical of bdi is formed as a result of fast photoinduced electron transfer processes from the excited state of the Ru^{II}(bpy) moiety to bdi. However, the emission data reveal the

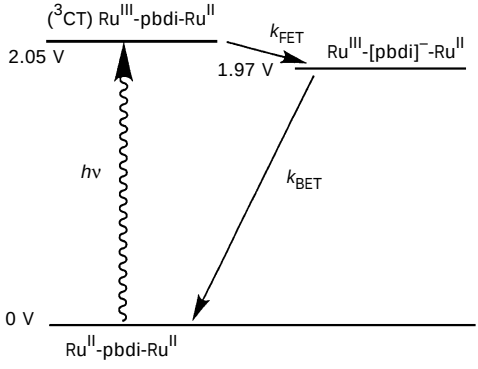

SCHEME 4

presence of additional slower-decay components (1.9 and 79 ns), suggesting the multiple conformations of this complex. Broadness of the absorption band of the anion radical of bdi and much shorter lifetime (50 ps) compared to the other components, suggest that the fastest electron transfer occurs within the conformer in which the bdi and Ru^{II}(bpy) moieties are in close contact. Thus, the bridging bdi anion radical was formed after photoirradiation as a result of photoinduced electron transfer form Ru^{II} to bdi (Fig. 7).

The propane-linker well established that several conformational isomers are present in solution[40]. Some of the possible conformers are shown in Scheme 3. In the studied $[\{Ru(bpy)_2\}_2(\mu\text{-pbdi})]^{4+}$ complex, the two Ru(II) centres repel each other and the molar excess of the expanded conformers (a), (b), or (c) in Scheme 3 may be large. Further, the distance between the Ru-bpy centre and the diimide moiety in the conformer (b) is almost the same as that in the conformer (c). As a result, the photoinduced electron transfer is governed by these two major conformers, as revealed by two kinetically different decay curves.

$[\{Ru(bpy)_2\}_2(\mu\text{-pndi})]^{4+}$

The oxidative quenching of the excited Ru(bpy) moiety in $[Ru(bpy)_2L]$ is feasible for this complex, with the Gibbs energy difference of –0.37 eV. The picosecond time-resolved absorption spectrum of $[\{Ru(bpy)_2\}_2(\mu\text{-pndi})]^{4+}$ in BuCN, recorded 15 ps after excitation, exhibits the bleaching of the MLCT band at 460 nm and the rise in absorption around 400 and 550 nm due to the radical anion of the bpy ligand, pointing to the formation of an ^{3}MLCT excited state of the $Ru(bpy)_2^{2+}$ moiety. In 200 ps, several absorption peaks appeared at 470, 610, 682 and 756 nm, which are characteristics of the anion radical of ndi[15] (Fig. 8). These new transient absorption peaks then disappeared in a single exponential decay to reproduce the ground state. The time profile reveals that the rise and decay times of the absorbance at 610 nm are 91 and 480 ps, respectively. The electron transfer rate constant (k_{ET}) is assumably calculated according to Eq. (*2*),

$$k_{ET} = \frac{1}{\tau} - \frac{1}{\tau_{model}}, \qquad (2)$$

where τ and τ_{model} are lifetimes of the complex of interest and a model complex, respectively. Thus, the rates of the photoinduced and the back elec-

tron transfers between the $Ru(bpy)_2$ moiety and bridging ndi for this complex are determined as $1.6 \cdot 10^{10}$ and $2.9 \cdot 10^9$ s^{-1}, respectively, as determined from the excited state decay and the charge separation yield.

Changing the substituent on the bpy ligand from R = H to CH_3, both forward and backward electron transfers become slightly faster. However, $[\{Ru(btfmb)_2\}_2(\mu\text{-pndi})]^{4+}$ in BuCN does emit and the photoinduced electron transfer processes are very slow ($k_{ET} = 3.8 \cdot 10^7$ s^{-1} from the emission lifetime), due to the localization of the excited electron almost exclusively on the btfmb ligand, compared with the existence of the excited electron both on the bridging ligand, the 2-(2-pyridyl)benzimidazole moiety, and the L′ ligand in the $[\{RuL'_2\}_2(\mu\text{-pndi})]^{4+}$ (L′ = bpy, dmbpy)[33] (Scheme 5).

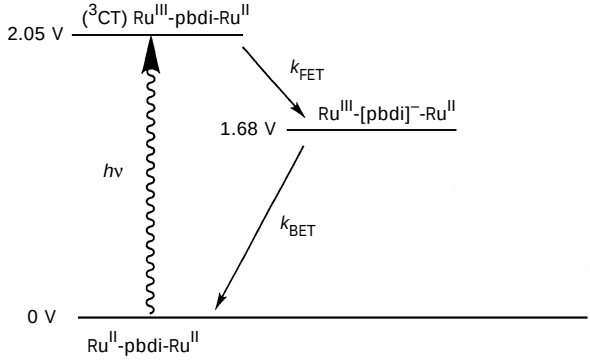

SCHEME 5

$[\{Os(bpy)_2\}_2(\mu\text{-pndi})]^{4+}$

In the $[\{Os(bpy)_2\}_2(\mu\text{-pndi})]^{4+}$ complex, the ^{3}MLCT excited state of the $Os(bpy)_2^{2+}$ moiety decayed faster than that of the corresponding diruthenium complex (rate is $2.7 \cdot 10^{10}$ s^{-1}), yielding the charge separated state (Os^{III}-[pndi]$^-$-Os^{II}) that was proved by the transient absorption spectra. The triple-exponential decay was also observed for this diosmium complex.

Other Dyads

The mononuclear complexes, $[M(bpy)_2L]^{2+}$ (M = Ru or Os; L = pbdi or pndi), behave nearly in the same way as the corresponding homodinuclear complexes $[\{M(bpy)_2\}_2(\mu\text{-L})]^{4+}$. The lifetime values and electron-transfer rates are collected in Table IV.

Photoinduced Electron-Transfer and Back Electron-Transfer Processes in Triad Complexes

$[Ru^{II}(bpy)_2(\mu\text{-pndi})Os^{II}(bpy)_2]^{4+}$

When the Ru^{II}-pndi-Os^{II} complex is excited with 400-nm light, two emission maxima are clearly observed around 650 and 750 nm. The emission is assigned to ^{3}MLCT excited states of $Ru(bpy)_2^{2+}$ and $Os(bpy)_2^{2+}$ moieties, respectively. The intensity of the emission from $Ru(bpy)_2^{2+}$ decreases faster

TABLE IV
Rate constants of photoinduced electron transfer reactions in mononuclear and dinuclear complexes, determined from picosecond transient absorption spectra in CH_3CN

Complex	Conditions[b]	FET rate from *M[c] ($\cdot 10^9$ s^{-1})	$-\Delta G_{FET}$[d] eV	Back ET rate[e] ($\cdot 10^9$ s^{-1})	$-\Delta G_{BET}$[f] eV
Mononuclear					
$[Ru(bpy)_2(pbdi)]^{2+}$	A	≈30[e], 16	0.08	≈5	1.97
$[Ru(bpy)_2(pndi)]^{2+}$	A	12	0.34	3.0	1.71
$[Ru(bpy)_2(mndi)]^{2+}$	A	18[c]	0.33	–	1.72
$[Os(bpy)_2(pndi)]^{2+}$	A	28[e], 14	0.39	8, 2.8	1.30
Dinuclear					
$[\{Ru(bpy)_2\}_2(\mu\text{-pbdi})]^{4+}$	A	≈18[e], 5.9	0.08	≈2	1.97
$[Ru(bpy)_2(\mu\text{-pbdi})Os(bpy)_2]^{5+}$	B	0.83	0.08	–	0.42
$[\{Ru(bpy)_2\}_2(\mu\text{-pndi})]^{4+}$	A	16	0.37	2.9	1.69
	B	12[e]	0.37	3.2	1.69
$[\{Ru(bpy)_2\}_2(\mu\text{-xndi})]^{4+}$	A	0.16	0.37	(not detected)	1.70
$[Ru(bpy)_2(\mu\text{-pndi})Os(bpy)_2]^{5+}$	B	23 (Ru)	0.37	0.0091[g]	0.42
$[Ru(bpy)_2(\mu\text{-xndi})Os(bpy)_2]^{4+}$	A	0.55[c]	0.37	–	1.69
$[\{Os(bpy)_2\}_2(\mu\text{-pndi})]^{4+}$	A	23	0.42	10, 2.8	1.27

[a] ndi = naphthalene-1,4:5,8-bis(dicarboximide) and bdi = pyromellitdiimide. [b] A = acetonitrile only, B = acetonitrile with 10^{-1} M $TBAClO_4$ as supporting electrolyte. [c] Gibbs energy change for the forward electron transfer. [d] Gibbs energy change for the back electron transfer. [e] Calculated from the first component of emission lifetimes, τ_1 in Table III . [f] From the transient absorption decay curve. Dynamic movement in the complexes reveals two different decays for $[Os(bpy)_2(pndi)]^{2+}$ and $[\{Os(bpy)_2\}_2(\mu\text{-pndi})]^{4+}$ due to the presence of different confomers. [g] Back ET rate for Ru(III)-Os(II)→Ru(II)-Os(III).

than that from the excited $Os(bpy)_2^{2+}$ moiety. Two quenching mechanisms may operate, *i.e.*, energy transfer and electron transfer. In the studied Ru-pndi-Os complex, the emission lifetime of the $Ru(bpy)_2$ moiety is the same as that of $[\{Ru(bpy)_2\}_2(\mu\text{-pndi})]^{4+}$. In addition, new absorption peaks at 470, 610, 682 and 756 nm due to the pndi radical anion arise in the transient absorption spectra after excitation, indicating that the energy transfer from excited $^*Ru(bpy)_2$ to $Os(bpy)_2$ is not the major pathway for the quenching. Therefore, the electron-transfer quenching mechanism is dominant for this heterodinuclear complex, though many examples have been reported for the energy transfer mechanism in the $Ru(bpy)_2$-linker-$Os(bpy)_2$ type complexes[8,41–43]. However, the quantitative analysis of the electron transfer event is too complex to determine the corresponding kinetic data in the system under study.

$[Ru^{II}(bpy)_2(\mu\text{-pndi})Os^{III}(bpy)_2]^{5+}$

The mixed-valent Ru^{II}-pndi-Os^{III} complex was selectively produced by quantitative oxidative electrolysis of $[Ru^{II}(bpy)_2(\mu\text{-pndi})Os^{II}(bpy)_2]^{4+}$ at +0.5 V in acetonitrile solution containing $1 \cdot 10^{-1}$ M $TBAClO_4$ (ref.[24]). The transient absorption spectrum of the mixed-valent complex, $[Ru^{II}(bpy)_2(\mu\text{-pndi})Os^{III}(bpy)_2]^{5+}$, reveals the formation of the Ru^{II}-to-bpy CT excited state directly after the excitation, as shown in Fig. 9. A tiny peak arose at 608 nm in 50 ps, followed by the appearance of absorption bands at 500 and 650 nm due to the Os^{II}-to-bpy CT excited state. The weak absorption at 608 nm, appearing only at the earliest stage, indicates formation of the anion radical of ndi. The fast electron transfer from this radical anion to the Os(III) site produces a charge-separated state, Ru^{III}-pndi-Os^{II}, which is the redox isomer state of the starting mixed-valent complex. The back electron transfer from the $[ndi]^-$ anion to the Ru(III) site would reduce the population of the charge-separated state, estimated to reach 75% on grounds of the transient absorption at 650 nm, using molar absorption coefficients of the model complexes $[^*Ru(bpy)_2L]^{2+}$ ($\Delta\varepsilon$ = –7 800 M^{-1} cm^{-1} at 460 nm), $[Ru(bpy)_2(L)]^{3+}$ (2 000 M^{-1} cm^{-1} at 650 nm), $[Os(bpy)_2(L)]^{2+}$ (3 500 M^{-1} cm^{-1} at 650 nm) and $[Os(bpy)_2(L)]^{3+}$ (780 M^{-1} cm^{-1} at 650 nm), where L = 1-methyl-2-(2-pyridyl)benzimidazole)[44]. Considering the similarity between the decay rate of the (^{3}CT)Ru excited state of Ru^{II}-pndi-Os^{III} for the complex $[Ru^{II}(bpy)_2(\mu\text{-pndi})Os^{III}(bpy)_2]^{5+}$ and that for the homodinuclear Ru complex, $[\{Ru(bpy)_2\}_2(\mu\text{-pndi})]^{4+}$, the electron transfer occurs first from Ru(II) to ndi, followed by rapid electron transfer from the radical anion of ndi to Os(III) (Scheme 6). The direct photoinduced electron-transfer process from

(^{3}CT)Ru to Os(III) is much slower than this stepwise electron transfer because the charge-separated state was not appreciably observed in Ru^{II}-pbdi-Os^{III} complex within 100 ps. The rate of back electron transfer from Os(II) to Ru(III) is calculated as $9.1 \cdot 10^6$ s^{-1} (τ = 110 ns) (Table IV). This slow charge recombination rate implies that the propane linker keeps

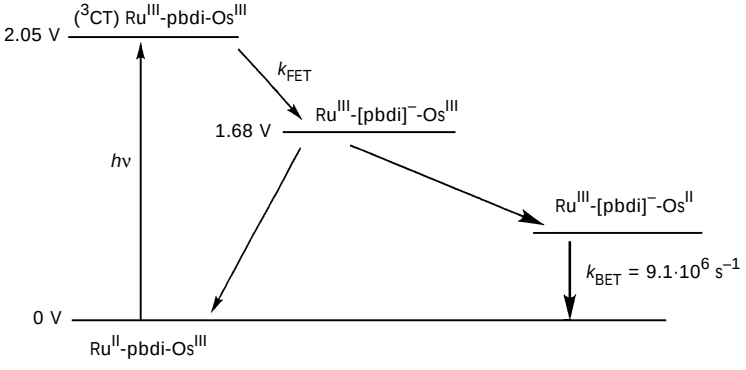

SCHEME 6

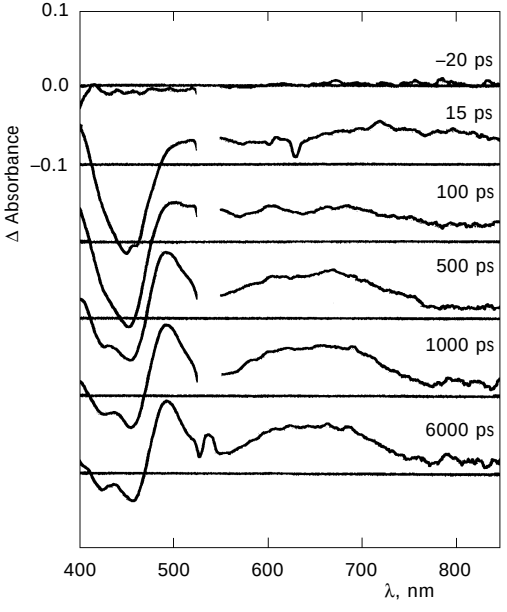

FIG. 9

Transient difference absorption spectra of the mixed-valence complex $[Ru^{II}(bpy)_2(\mu\text{-pndi})\text{-}Os^{III}(bpy)_2]^{5+}$, generated in an electrochemical flow cell in CH_3CN ($3 \cdot 10^{-4}$ M with $1 \cdot 10^{-1}$ M $TBABF_4$ as supporting electrolyte) at room temperature

the Ru(III) and Os(II) moieties apart from each other. The Ru–Os distance is estimated as ≈21 Å from the optimized molecular geometry.

Dependence of Photoinduced Electron-Transfer Processes on Linker Groups

$[Ru^{II}(bpy)_2(\mu\text{-xndi})Os^{III}(bpy)_2]^{5+}$

In order to elucidate the distance and conformational dependence in Ru/Os-diimide complexes, the linker group between $M(bpy)_2L$ and diimide was changed from propane to *p*-xylene (see Scheme 1; the ndi and bdi bridges are now abbreviated as xndi and xbdi, respectively). Due to this change, the rate of electron transfer from $Ru(bpy)_2$ to xndi becomes slow. From the viewpoint of the Gibbs energy differences, the values are the same. From the molecular modeling, the centre-to-centre distance between the Ru moiety and ndi in the extended conformer is ≈10 Å for the propane linker (pndi) and ≈17 Å for the *p*-xylene one (xndi). The distance between Ru and ndi is the most important factor for the photoinduced electron transfer in the present Ru-diimide system. Furthermore, the conformational rigidity is higher for the *p*-xylene linker, even though several conformers can be considered.

Conclusion

In conclusion, we have prepared and characterized a series of mono- and dinuclear Ru/Os complexes containing a bridging ligand, L-diimide-L (L = 2-(2-pyridyl)benzimidazole, diimide = pyromellitimide (bdi) or naphthalene-1,4:5,8-bis(dicarboximide) (ndi)) with different linkers. The photoinduced electron transfer from the $M(bpy)_2$ moiety (M = Ru or Os) to the diimide site takes place, involving several pathways within the conformational isomers in solution. The electron-transfer rates decrease in the order of pndi > pbdi ≈ xndi > xbdi when changing the linker and diimide. The dinuclear complexes prefer an extended conformation because of coulombic repulsion between the cationic $M(bpy)_2$ groups. On the other hand, the charge transfer interaction between $M(bpy)_2$ and diimide is possible, leading to a folded conformation[19,45]. These two conformers are involved in the electron transfer event in the dinuclear dyad and triad complexes under study, as the rotation about the C–C bond is slower compared with the lifetime of the charge-separated state in the studied system. However, controlling dynamic movement between the folded and ex-

tended conformations through the linker part will become a target towards the light-driven molecular actuator in the future.

M. H. gratefully acknowledges financial support from the Ministry of Education, Science, Sports and Culture by a "Grant-in-Aid for Scientific Research" (No. 12440188), a "Grant-in-Aid for Scientific Research on Priority Areas of Metal-assembled Complexes and Creation of Delocalized Electronic Systems" (No. 10146103), and also support from the Promotion and Mutual Aid Corporation for Private Schools of Japan. M. D. H. also acknowledges the Ministry of Education for a Japanese Government (Monbusho) Scholarship.

REFERENCES

1. Bixon M., Jortner J.: *Adv. Chem. Phys.* **1999**, *106*, 35.
2. Gust D., Moore T. A.: *Top. Curr. Chem.* **1991**, *159*, 105.
3. Wasielewski M. R.: *Chem. Rev. (Washington, D. C.)* **1992**, *92*, 435.
4. Osuka A., Nakajima S., Okada T., Taniguchi S., Nozaki K., Ohno T., Yamazaki I., Nishimura Y., Mataga N.: *Angew. Chem., Int. Ed. Engl.* **1996**, *35*, 92.
5. Fox M. A., Jones W. E., Watkins D. M.: *Chem. Eng. News* **1993**, 38.
6. Mataga N., Miyasak, H.: *Adv. Chem. Phys.* **1999**, *107*, 431.
7. Balzani V., Juris A., Venturi S., Campagna S., Serroni S.: *Chem. Rev. (Washington, D. C.)* **1996**, *96*, 759.
8. Balzani V., Campagna S., Denti G., Juris A., Serroni S., Venturi M.: *Acc. Chem. Res.* **1998**, *31*, 26.
9. Mecklenburg S. L., Peek B. M., Schoonover J. R., McCafferty D. G., Wall C. G., Erickson B. W., Meyer T. J.: *J. Am. Chem. Soc.* **1993**, *115*, 5479.
10. Yonemoto E. H., Saupe G. B., Schmehl R. H., Hubig S. M., Riley R. L., Iverson B. L., Mallouk T. E.: *J. Am. Chem. Soc.* **1994**, *116*, 4786.
11. Gulyas P. T., Smith T. A., Paddon-Row M. N.: *J. Chem. Soc., Dalton Trans.* **1999**, 1325.
12. Debreczeny M. P., Svec W. A., Wasielewski M. R.: *Science* **1996**, *274*, 584.
13. Osuka A., Marumo S., Maruyama K., Mataga N., Tanaka Y., Taniguchi S., Okada T., Yamazaki I., Nishimura Y.: *Bull. Chem. Soc. Jpn.* **1995**, *68*, 262.
14. O'Neil M. P., Niemczyk M. P., Svec W. A., Gosztola D., Gaines III G. L., Wasielewski M. R.: *Science* **1992**, *257*, 63.
15. Osuka A., Zhang R.-P., Maruyama K., Ohno T., Nozaki K.: *Bull. Chem. Soc. Jpn.* **1993**, *66*, 3773.
16. Nagata T.: *Bull. Chem. Soc. Jpn.* **1991**, *64*, 3005.
17. Wirderrecht G. P., Niemczyk M. P., Svec W. A., Wasielewski M. R.: *J. Am. Chem. Soc.* **1996**, *118*, 81.
18. Green S., Fox M. A.: *J. Phys. Chem.* **1995**, *99*, 14752.
19. Steullet V., Dixon D. W.: *J. Chem. Soc., Perkin Trans. 2* **1999**, 1547.
20. Dixon D. W., Thornton N. B., Steullet V., Netzel T.: *Inorg. Chem.* **1999**, *38*, 5526.
21. Takenaka S., Yokoyama M., Kondo H.: *Chem. Commun.* **1997**, 115.
22. Hamilton D. G., Sanders K. M., Davies J. E., Cleg W., Teat S. *J.: Chem. Commun.* **1997**, 897.
23. Houghton M. A., Bilyk A., Harding M. M., Turner P., Hambley T. W.: *J. Chem. Soc., Dalton Trans.* **1997**, 2725.

24. Hossain M. D., Haga M., Monjushiro H., Gholamkhass B., Nozaki K., Ohno T.: *Chem. Lett.* **1997**, 573.
25. Walter J. L., Freiser H.: *Anal. Chem.* **1954**, *26*, 217.
26. Furue M., Maruyama K., Ogumi T., Naiki M., Kamachi M.: *Inorg. Chem.* **1992**, *31*, 3792.
27. Lay P. A., Sargeson A., Taube H.: *Inorg. Synth.* **1986**, 24, 291.
28. Haga M., Matsumura-Inoue T., Yamabe S.: *Inorg. Chem.* **1987**, *26*, 4148.
29. Ohno T., Nozaki K., Haga M.: *Inorg. Chem.* **1992**, *31*, 548.
30. Tsushima M., Ikeda N., Nozaki K., Ohno T.: *J. Phys. Chem.* **2000**, *104*, 5176.
31. Yoshimura A., Nozaki K., Ikeda N., Ohno T.: *J. Phys. Chem.* **1996**, *100*, 1630.
32. Haga M., Ano T., Kano K., Yamabe S.: *Inorg. Chem.* **1991**, *30*, 3843.
33. Ohno T., Nozaki K., Haga M.: *Inorg. Chem.* **1992**, *31*, 4256.
34. Haga M., Ano T., Ishizaki T., Kano K., Nozaki K., Ohno T.: *J. Chem. Soc., Dalton Trans.* **1994**, 263.
35. Haga M., Ali M. M., Maegawa H., Nozaki K., Yoshimura A., Ohno T.: *Coord. Chem. Rev.* **1994**, *132*, 99.
36. Adachi M., Murata Y., Nakamura S.: *J. Phys. Chem.* **1995**, *99*, 14240.
37. Richardson D. E., Taube H.: *Inorg. Chem.* **1981**, *20*, 1278.
38. Haga M.: *Inorg. Chim. Acta* **1983**, *75*, 29.
39. Gholamkhass B., Nozaki K., Ohno T.: *J. Phys. Chem. B* **1997**, *101*, 9010.
40. Zachariasse K. A., Duveneck G., Huhnle W., Leinhos U., Reynders P. in: *Photochemical Processes in Organized Molecular Systems* (K. Honda, Ed.), p. 83. Elsevier, North-Holland 1991.
41. Furue M., Yoshidzumi T., Kinoshita S., Kushida T., Nozakura S., Kamachi M.: *Bull. Chem. Soc. Jpn.* **1991**, *64*, 1632.
42. Brewer K. J.: *Comments Inorg. Chem.* **1999**, *21*, 201.
43. Barigelletti F., Flamigni L., Collin J.-P., Sauvage J.-P.: *Chem. Commun.* **1997**, 333.
44. Nozaki K., Ikeda N., Ohno T.: *New J. Chem.* **1996**, *20*, 739.
45. Berg-Brennan C. A., Yoon D. I., Slone R. V., Kazala A. P., Hupp J. T.: *Inorg. Chem.* **1996**, *35*, 2032.